

# Supporting Information

## **Polyhedron-Assembled Ternary PtCuCo Nanochains: Integrated Functions Enhance the Electrocatalytic Performance of Methanol Oxidation at Elevated Temperature**

*Bin Luo,<sup>a</sup> Fengling Zhao,<sup>a</sup> Zixuan Xie,<sup>a</sup> Qiang Yuan,<sup>\*a, b</sup> Fang Yang,<sup>a</sup> Xiaotong Yang,<sup>a</sup> Chaozhong Li,<sup>a</sup> Zhiyou Zhou<sup>c</sup>*

<sup>a</sup>Department of Chemistry, College of Chemistry and Chemical Engineering, Guizhou University, Guiyang, Guizhou province 550025, P. R. China.

<sup>b</sup>Key Lab of Organic Optoelectronics & Molecular Engineering, Tsinghua University, Beijing 100084, P. R. China.

<sup>c</sup>State Key Laboratory of Physical Chemistry of Solid Surfaces, College of Chemistry and Chemical Engineering, Xiamen University, Xiamen 361005, P. R. China.

**Corresponding Author**

E-mail: qyuan@gzu.edu.cn

**Characterizations:** The size and morphology of the nanochains were determined by a HITACHI H-7700 transmission electron microscope (TEM) at 100 kV, and a FEI Tecnai G2 F20 S-Twin high-resolution transmission electron microscope (HRTEM) equipped with energy dispersive spectrometer (EDS) analyses at 200 kV. The high-angle annular dark-field scanning TEM (HAADF-STEM) was determined by a FEI Tecnai G2 F20 S-Twin HRTEM operating at 200 kV. The scanning electron microscope (SEM) image was performed with SIGMA+X-Max20 instrument equipped with energy dispersive spectrometer (EDS) analyses. The X-ray diffraction (XRD) patterns were performed on a Bruker D8 ADVANCE X-ray powder diffractometer operated at 40 kV voltage and 40 mA current with Cu K $\alpha$  radiation ( $\lambda = 1.5418 \text{ \AA}$ ). X-ray photoelectron spectroscopy (XPS) measurements were performed using a PHI Quantum 2000 Scanning ESCA Microprobe (Physical Electronics, USA), using Al K $\alpha$  X-ray radiation (1486.6 eV) for excitation. Binding energies were corrected from charge effects by reference to the C1s peak of carbon at 284.8 eV. The inductively coupled plasma optical emission spectrometry (ICP-OES) analysis of samples was performed on IRIS Intrepid II XSP (ThermoFisher).

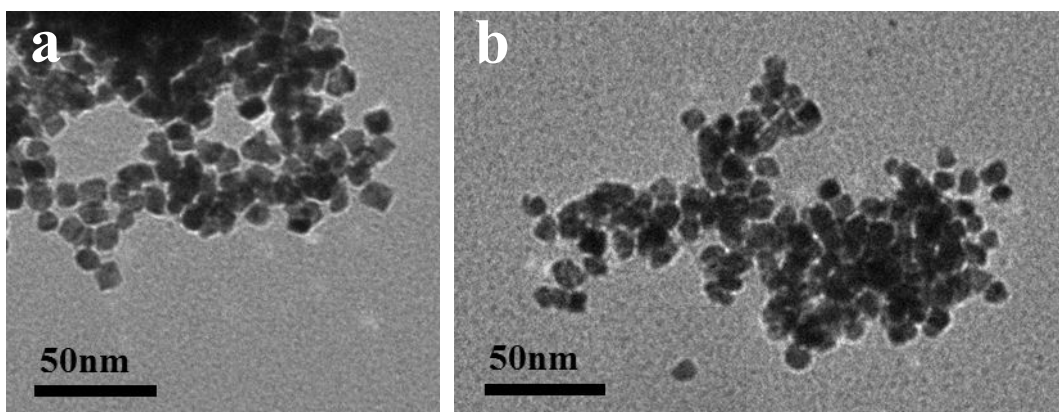


**Figure S1.** TEM images of PtCuCo products synthesized with the same synthesis procedure of  $\text{Pt}_{45}\text{Cu}_{35}\text{Co}_{20}$  at 2 h.

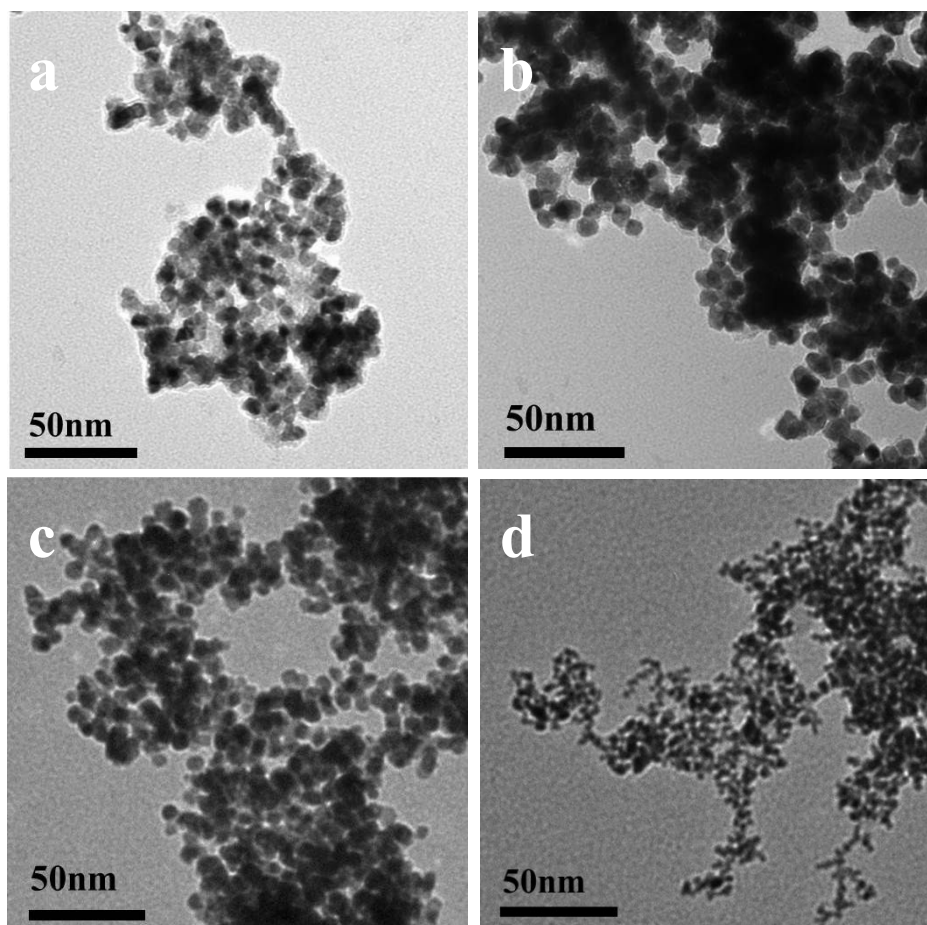


**Figure S2.** TEM images of PtCuCo nanochains and PtCu nanochains synthesized with the same procedure. (a)  $\text{Pt}_{36}\text{Cu}_{49}\text{Co}_{15}$ ; (b)  $\text{Pt}_{35}\text{Cu}_{30}\text{Co}_{35}$ ; (c)  $\text{Pt}_{66}\text{Cu}_{34}$  and (d)  $\text{Pt}_{94}\text{Co}_6$ .

**Table S1.** The inductively coupled plasma optical emission spectrometer (ICP-OES) results for as-synthesized PtCuCo and PtCu nanochains.

Sample	Element	Atomic% Feeding ratio	Atomic% (result from ICP-OES)
Pt <sub>45</sub> Cu <sub>35</sub> Co <sub>20</sub>	Pt	33.4	45
	Cu	33.3	35
	Co	33.3	20
Pt <sub>36</sub> Cu <sub>49</sub> Co <sub>15</sub>	Pt	25	36
	Cu	50	49
	Co	25	15
Pt <sub>35</sub> Cu <sub>30</sub> Co <sub>35</sub>	Pt	25	35
	Cu	25	30
	Co	50	35
Pt <sub>66</sub> Cu <sub>34</sub>	Pt	50	66
	Cu	50	34
Pt <sub>94</sub> Co <sub>6</sub>	Pt	50	94
	Co	50	6

**Table S2.** XRD informations of different samples.

Samples	2 $\theta$ /degree (111)	Lattice parameter (Å)	d <sub>(111)</sub> spacing (nm)	Strain (%)
Pt (JCPDS-04-0802)	39.76	3.923	0.2265	
Pt <sub>45</sub> Cu <sub>35</sub> Co <sub>20</sub>	40.96	3.816	0.2203	2.74
Pt <sub>36</sub> Cu <sub>49</sub> Co <sub>15</sub>	41.18	3.797	0.2192	3.22
Pt <sub>35</sub> Cu <sub>30</sub> Co <sub>35</sub>	41.28	3.788	0.2187	3.44
Pt <sub>66</sub> Cu <sub>34</sub>	40.86	3.825	0.2208	2.52
Pt <sub>94</sub> Co <sub>6</sub>	39.99	3.905	0.2255	0.44

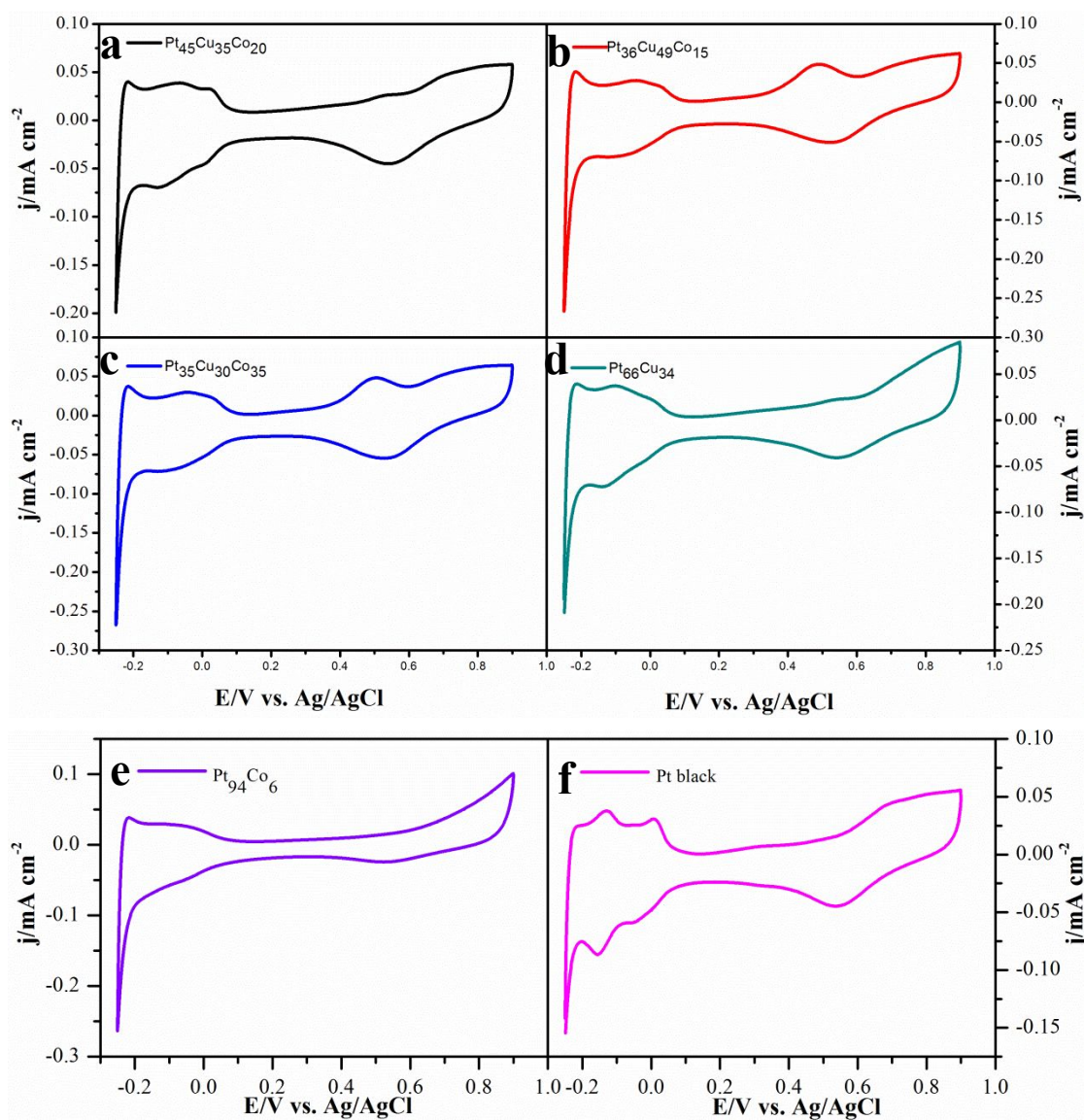


**Figure S3.** Cyclic voltammetry (CV) curves of (a)  $\text{Pt}_{45}\text{Cu}_{35}\text{Co}_{20}$ , (b)  $\text{Pt}_{36}\text{Cu}_{49}\text{Co}_{15}$ , (c)  $\text{Pt}_{35}\text{Cu}_{30}\text{Co}_{35}$ , (d)  $\text{Pt}_{66}\text{Cu}_{34}$  nanochains, (e)  $\text{Pt}_{94}\text{Co}_6$  nanochains and (f) commercial Pt black in  $\text{N}_2$ -saturated 0.1 M  $\text{H}_2\text{SO}_4$  solution at room temperature.

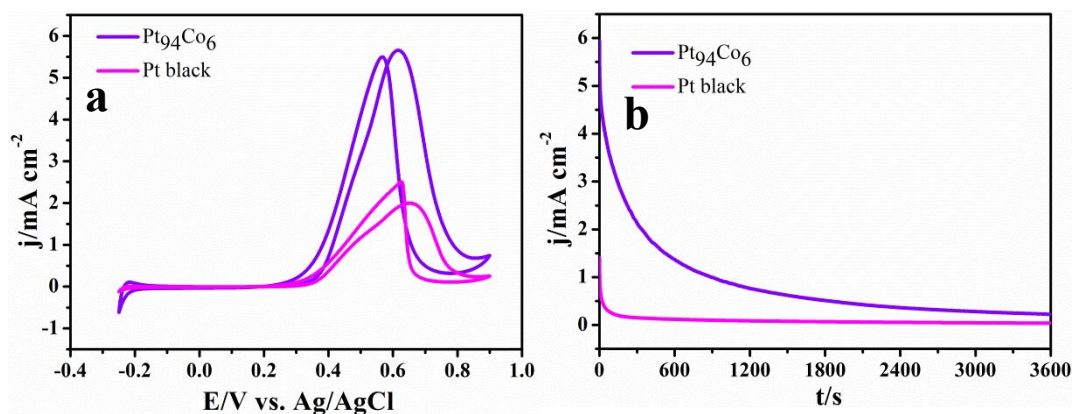


**Figure S4.** (a) CV curves of the synthesized  $\text{Pt}_{94}\text{Co}_6$  nanochains and commercial Pt black, scanning rate  $50 \text{ mV s}^{-1}$ , in  $0.1 \text{ M H}_2\text{SO}_4 + 0.5 \text{ M CH}_3\text{OH}$  solution at  $60^\circ\text{C}$ . (b) Current-time (i-t) curves recorded at  $0.6 \text{ V}$  for  $3600$  seconds.

**Table S3.** Summaries of MOR activity of the prepare nanochains and commercial Pt black in  $0.1 \text{ M H}_2\text{SO}_4 + 0.5 \text{ M CH}_3\text{OH}$  solution at  $60^\circ\text{C}$ .

Sample	ECSA ( $\text{m}^2/\text{g}_{\text{Pt}}$ )	Specific activity ( $\text{mA}/\text{cm}^2$ )	Mass activity ( $\text{A}/\text{mg}$ )	Specific activity improvement factor (vs. Pt black)	Mass activity improvement factor (vs. Pt black)
$\text{Pt}_{45}\text{Cu}_{35}\text{Co}_{20}$	23.00	18.24	4.19	9.25	10.47
$\text{Pt}_{36}\text{Cu}_{49}\text{Co}_{15}$	21.70	14.28	3.10	7.24	7.75
$\text{Pt}_{35}\text{Cu}_{30}\text{Co}_{35}$	21.10	10.64	2.25	5.40	5.62
$\text{Pt}_{66}\text{Cu}_{34}$	20.50	11.96	2.45	6.07	6.12
$\text{Pt}_{94}\text{Co}_6$	18.55	5.66	1.05	2.87	2.63
Pt black	20.00	1.97	0.40	1	1

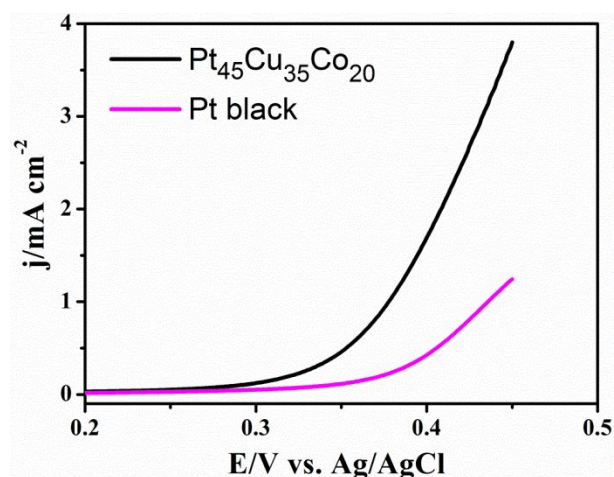


**Figure S5.** Linear sweep voltammetry curves of  $\text{Pt}_{45}\text{Cu}_{35}\text{Co}_{20}$  nanochains commercial Pt black measured with a scan rate of  $50 \text{ mV s}^{-1}$  in a solution of  $0.1 \text{ M H}_2\text{SO}_4 + 0.5 \text{ M CH}_3\text{OH}$  at  $60^\circ\text{C}$ .

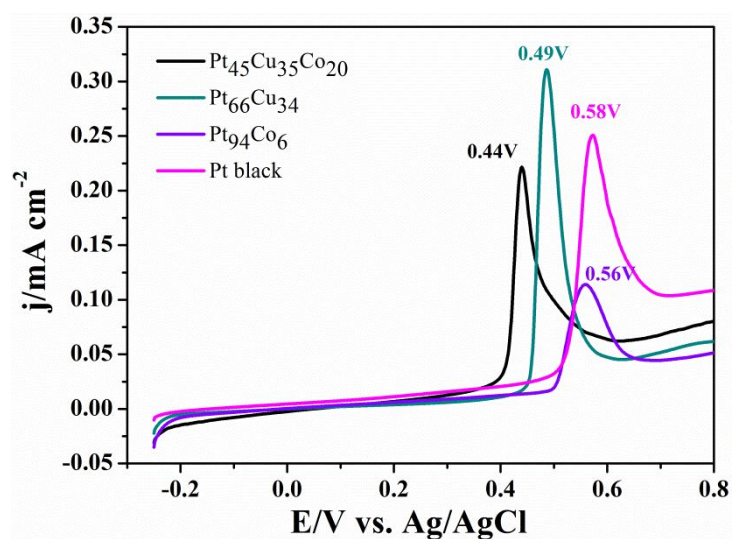


**Figure S6.** LSV curves of CO stripping test of  $\text{Pt}_{45}\text{Cu}_{35}\text{Co}_{20}$  nanochains,  $\text{Pt}_{66}\text{Cu}_{34}$  nanochains,  $\text{Pt}_{94}\text{Co}_6$  nanochains and commercial Pt black in CO-saturated  $0.1 \text{ M H}_2\text{SO}_4$  solution at  $60^\circ\text{C}$  with a scanning rate of  $50 \text{ mV s}^{-1}$ .



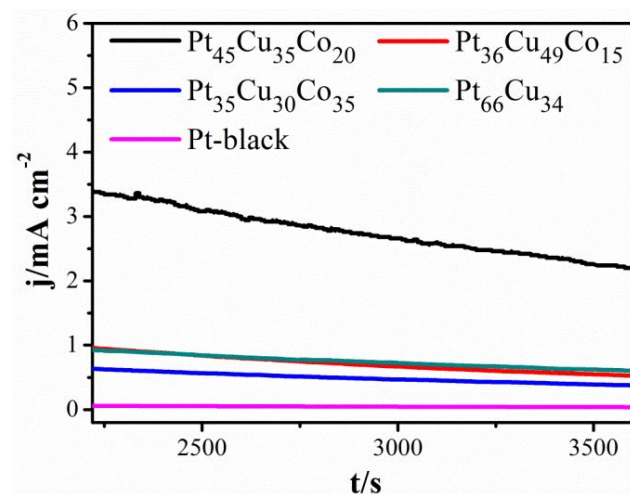


**Figure S7.** The current-time curves (2250 s-3600 s) of the synthesized  $\text{Pt}_{45}\text{Cu}_{35}\text{Co}_{20}$ ,  $\text{Pt}_{36}\text{Cu}_{49}\text{Co}_{15}$ ,  $\text{Pt}_{35}\text{Cu}_{30}\text{Co}_{35}$ ,  $\text{Pt}_{66}\text{Cu}_{34}$  nanochains and commercial Pt black at 0.6 V.

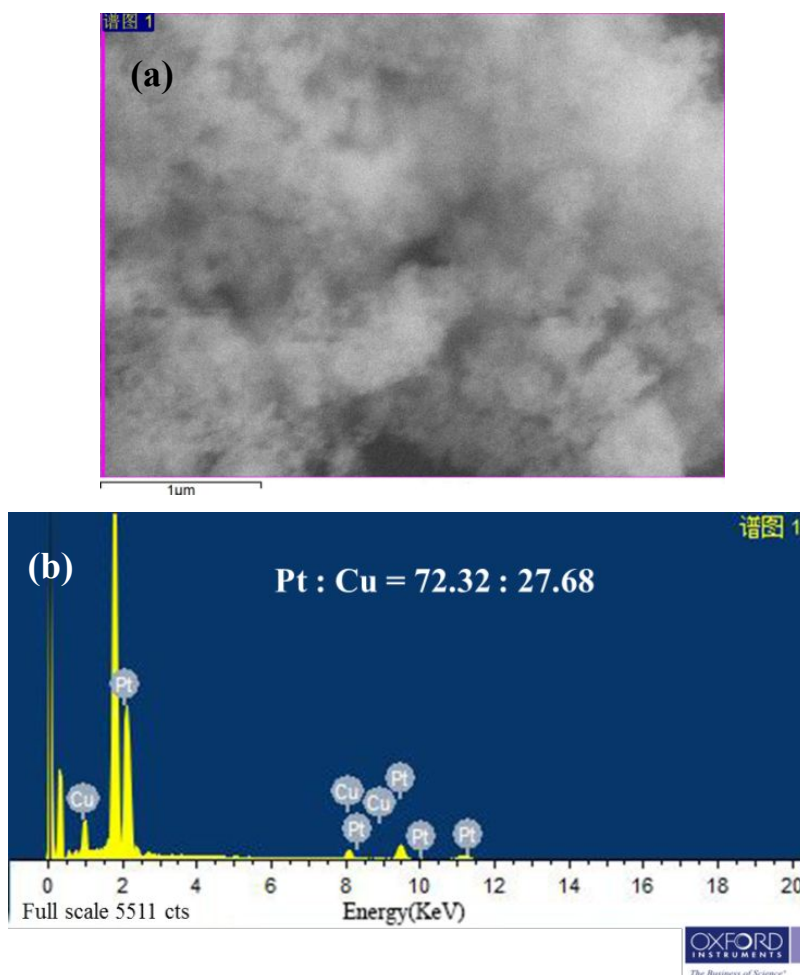


**Figure S8.** The SEM image (a) and corresponding EDS (b) of  $\text{Pt}_{45}\text{Cu}_{35}\text{Co}_{20}$  nanochains after 1 h durability test. (The result of EDS showed that the Cu and Co were obviously lost, specially for Co, the signals of Co can not be detected.)



Equation S1:

$$j_p = 0.4463(F^3/RT)^{1/2} n^{3/2} A D_0^{1/2} C_0^* v^{1/2}$$

In an electrooxidation reaction, if the relationship between the peak SA ( $j_p$ ) and the square root of sweep speed ( $v^{1/2}$ ) obeys the aforementioned equation (book: ELECTROCHEMICAL METHODS-Fundamentals and Applications. Allen J. Bard, Larry R. Faulkner, 2001, John Wiley & Sons, Inc. Chapter 6, Page 231.), then this reaction can be ascribed as a diffusion-controlled process.

In the equation, F is the Faraday constant; R is the gas constant; T is the absolute temperature of the reaction; n is the total number of electrons that are involved in the reactions; A is the surface area of the electrode, which is a constant;  $D_0$  is the diffusion coefficient;  $C_0^*$  is the pristine concentration of the reactant. For the electrooxidation reaction under the same conditions,  $C_0^*$  and  $D_0$  are the same. Thereby, the slope of  $j_p$  versus  $v^{1/2}$  is decided by  $n^{3/2}$ , and  $n^{3/2}$  is in connection with the electron transfer in the electrooxidation reaction, therefore, the bigger value of slope shows the enhanced kinetics.